WITHDRAWN: Regulatory T cells enhance stem-like characteristics of hepatocellular carcinoma cells through Wnt/β-catenin pathway

Chang Liu

bbtslp@126.com

Dalian Municipal Central Hospital https://orcid.org/0000-0002-3445-3134

Yan-yan Pan

Dalian Municipal Central Hospital Affiliated of Dalian Medical University

Jun Ji

Dalian Municipal Central Hospital Affiliated of Dalian Medical University

Yuan-yuan Wu

Dalian Municipal Central Hospital Affiliated of Dalian Medical University

He-shuang Wang

Dalian Municipal Central Hospital Affiliated of Dalian Medical University

Yan-yan Gao

Dalian Municipal Central Hospital Affiliated of Dalian Medical University

Li Zhang

Dalian Municipal Central Hospital Affiliated of Dalian Medical University

Research

Keywords: Exosomes, Tumor initiating cells, Cancer stem cells, FoxP3, CD133

Posted Date: November 23rd, 2020

DOI: https://doi.org/10.21203/rs.3.rs-111229/v1

EDITORIAL NOTE:

The full text of this preprint has been withdrawn by the authors while they make corrections to the work. Therefore, the authors do not wish this work to be cited as a reference. Questions should be directed to the corresponding author.

Abstract

Background: Tumor initiating cells (TICs) were confirmed to drive the therapeutic resistance of hepatocellular carcinoma (HCC), but the mechanism by which tumor microenvironment maintains the HCC stemness is not fully understood. This study aims to investigate the effect of regulatory T cells (Tregs) on the TICs characteristics of HCC.

Methods: Immunocytochemistry, flow cytometry, real-time PCR, western blot, in vitro sphere-formation, and in vivo tumorigenesis assay were used to detect HCC TIC characteristics. Additionally, the association between FoxP3 expression, Wnt/β-catenin pathway activation, and HCC stemness were analyzed by forced expression or inhibition of FoxP3.

Results: It was showed Tregs enhanced the stemness of HCC cells by upregulation of TIC-related markers CD133, Oct3/4, Sox2, c-Myc, Klf4, Nanog, CD13, EpCAM, and induction of epithelial to mesenchymal transition (EMT), increase of TICs ratio, as well as promotion of tumorigenic ability. Moreover, β-catenin and c-Myc were upregulated in HCC cells when co-cultured with Tregs. After Wnt/β-catenin pathway inhibition, HCC stemness was also inhibited. In addition, Tregs-derived exosomes played the same role as Tregs in enhancing HCC TIC properties, and exosome inhibition led to decreased TIC ratio as well as TIC markers expression. Furthermore, Tregs-derived exosomes down-regulate FoxP3 and GSK3β of HCC cells. Forced expression of FoxP3 resulted in increased GSK3β, decreased β-catenin and TIC ratio of HCC. In contrast, FoxP3 interference reduced GSK3β, increased β-catenin and TIC ratio.

Conclusions: This study, for the first time, demonstrated Tregs enhanced HCC stemness through Wnt//β-catenin pathway by down-regulating FoxP3.

Background

HCC is the most prevalent primary liver cancer, which ranks as the six most common cancers and second most leading cause of cancer-related death worldwide. Higher incidence rate of hepatitis B virus occurs in China, and over 50% of HCC related death is in China [1]. Late diagnosis, frequent relapse and the refractory nature to chemotherapy render HCC intractable.

Due to the inherently high genetic instability, a small population within the HCC was evolved with the ability of initiation and maintenance of cancer growth. Rapidly growing evidence has demonstrated that some HCCs, if not all, were caused by the activation of the TICs, their resistance to anticancer drugs is an obstacle for the total eradication of HCC [2]. The extraordinary capacities of self-renewal, tumorigenicity and differentiation endow TICs a pivotal role in tumor relapse, therapy resistance, and metastasis. TICs typically harbor persistent activation of highly conserved stemness signaling pathways including Wnt/β-catenin, Hedgehog, Notch. Wnt/β-catenin signaling has been reported to be one of the most active signaling pathways indispensable to self-renewal and drug-resistance of TICs [3].

Tregs are a subset of $CD4^+CD25^+CD127^-$ T lymphocytes which constitutively express the transcription factor FoxP3 (forkhead box P3). Activated Tregs inhibit different subsets of immune cells via contact-dependent ways between checkpoint molecules and their ligands involving PD-1, PD-L1, CTLA-4, GITR, Tim-3, and galectin-9 [4]. Tregs have been shown to increase with tumor stage and correlate with poor prognosis in HCC [5, 6]. Nevertheless, the role of Tregs in regulation of HCC cellular behavior, including proliferation, metastasis, especially TICs characteristics, was undetermined. In the current study, we showed that Tregs promoted the stemness of HCC by down-regulation of FoxP3, and activation of Wnt/β-catenin pathway.

Methods

Materials

All chemicals were purchased from Sigma-Aldrich (St. Louis, MO, USA) unless otherwise specified. Sodium alginate (Qingdao Jingyan Bio-Tech, Qingdao, China) was purified by removing protein and endotoxin, according to the protocol used in our laboratory. XAV-939 and GW4869 were purchased from MedChemExpress (Monmouth Junction, NJ, USA).

Human sample

The use of human subjects was reviewed and approved by the Ethics Committee of Dalian Municipal Central Hospital. Mononuclear cells were isolated from the peripheral blood of a HCC patient by gradient centrifugation with lymphocytes separation medium (Lymphoprep, 08751, STEMCELL Techbology, Vancouver, BC, Canada).

Tregs isolation

Tregs were isolated from peripheral blood of a HCC patient, by $CD4^+$ $CD25^+CD127^{dim/-}$ Regulatory T Cell Isolation Kit (130-094-775, Miltenyi Biotec, Bergisch Gladbach, Germany). Briefly, the isolation of $CD4^+$ $CD25^+$ $CD127^{dim/-}$ regulatory T cells was performed with a cocktail of biotinylated antibodies and anti-Biotin microbeads for the depletion of non-$CD4^+$ and $CD127^{high}$ cells. Then the flow-through fraction of pre-enriched $CD4^+$ $CD127^{dim/-}$ T cells is labeled with CD25 microbeads for subsequent positive selection of $CD4^+CD25^+CD127^{dim/-}$ regulatory T cells with MidiMACS™ Starting Kit (Miltenyi Biotec).

Tregs were cultured in X-VIVO^{TM} 15 medium (BE02-060F, Lonza, Basel, Switzerland) supplemented with 2% heat-activated patient serum, 500 U/mL recombinant human IL-2 (T&L Biological Technology, Beijing, China), MACSiBead pre-loaded with CD3 and CD28 antibodies (130-095-353, Miltenyi Biotec), and 10 ng/ml rapamycin (HY-10219, MedChemExpress).

HCC cell culture, encapsulation and co-culture

Human HCC cell line MHCC-LM3, purchased from Cellcook (Cellcook biotech company, Guangzhou, China), were cultured in high glucose Dulbecco's Modified Eagle's Medium (H-DMEM, Invitrogen, Carlsbad, CA, USA) supplemented with 10% Fetal Bovine Serum (FBS, Invitrogen) in a 37 °C incubator with an atmosphere of 5% CO_2.

Single cells dissociated from monolayer cultures were counted and suspended in 1.5%, (w/v) sodium alginate at a cell density of 1×10^6/ml. The cell suspension was extruded into 100 mM $CaCl_2$ solution. The gelation time to produce calcium alginate gel (ALG) beads was 30 min. The encapsulated MHCC-LM3 cells were co-cultured with Tregs for 3 days in H-DMEM supplemented with 10 % FBS. Then Tregs were removed by sedimentation and filtration with 100 μm strainer (352360, Corning, NY, USA). The encapsulated HCC cells were harvested from ALG beads by treating with 55 mM sodium citrate, and then used for further experiments.

Plasmid, shRNAs and cell transfection

The plasmids for generating vectors were prepared from p-CMV-GreenZeo (Genechem, Shanghai, China). Short-hairpin small interfering RNA sequences were 5'-GAAGCAGCGGACACTCAAT-3', 5'-ACACGCATGTTTGCCTTC'.T-3', and 5'-TGGCAAATGGTGTCTGCAA-3'. A scrambled sequence (5'-TGACGCGATACGTATTGTA-3') was used as a negative control. Transfection of MHCC-LM3 cells were performed using Lipofectamine 3000 (Invitrogen). DNA-liposome complexes were prepared at 4˚C to a final volume of 1 μg/μl and added to MHCC-LM3 cells (1 μg/ml). Transfection was performed for 6 h at 37 °C.

Flow cytometry

Tregs were labeled with FITC Mouse Anti-Human CD4 (1:100), PE Mouse Anti-Human CD25 (1:200) and Alexa Fluor® 647 Mouse anti-Human FoxP3 (1:250) antibodies for 30 minutes on ice, followed by washing with phosphate buffered saline (PBS) (Gibco, Grand Island, NY, USA), FITC Mouse IgG1 (556649, BD Biosciences), PE Mouse IgG1 (5557449, BD Biosciences), Alexa Fluor® 647 Mouse IgG1 (557732, BD Biosciences) were used as isotype controls. As for FoxP3 staining, Human FoxP3 Buffer Set (560098, BD Biosciences) was used. Briefly, Tregs were fixed with Buffer A, incubated for 10 minutes at RT, and permeabilized with buffer C, incubated for 30 minutes at RT. Flow cytometry was performed by FACSCanto II flow cytometer, and the data were analyzed and presented using Flowjo software version 10 (Flowjo LLC, Ashland, OR, USA).

Quantitative reverse transcription polymerase chain reaction (RT-qPCR)

RT-qPCR (two-step method) was applied to examine the relative levels of the genes, using GAPDH as an internal control. The total RNA was isolated using TRIzol® reagent (Invitrogen), according to the manufacturer's instructions. Reverse transcription (RT) was performed using a PrimeScript RT Reagent Kit (RR036A, TaKaRa, Shiga, Japan). Real-time PCR was carried out with SYBR Premix Ex Taq (Perfect Real Time) (RR820A, Takara). PCR amplification and fluorescence detection were performed using a

LightCycler® 96 System (Roche, Basel, Swiss). The primers used in this study were listed in Table S. The results were presented as the calculated comparative expression ratios of target sample to control group for each sample using the Ct method (2-ΔΔ Ct).

Immunofluorescence staining

MHCC-LM3 cell spheres were fixed with 4% paraformaldehyde (PFA) (Sigma-Aldrich, Munich, Germany) and washed with PBS (Gibco) for three times. After cytospining, cells were treated with 0.05% Triton-X 100 (Sigma-Aldrich), then incubated with CD133 primary antibody (1:400) (64326, Cell Signaling Technology, Danvers, MA, USA) in PBS containing 1% goat serum (16210064, Thermal Fisher Scientific, Waltham, MA) at 4 °C overnight. Then the cells were treated with Alexa Fluor® 555 conjugated anti-rabbit IgG antibody (1:1000) (4413, Cell Signaling Technology) for 60 minutes at room temperature. The primary antibody was omitted for negative control. Nuclear staining was performed using Hoechst 33342 (H3570, Thermal Fisher Scientific). The samples were observed using an inverted fluorescence microscope (DMI8, Leica, Solms, Germany).

Western blot

Cells were lysed in lysis buffer containing protease and phosphatase inhibitors (Keygentec, Nanjing, China). Protein concentration was quantified by BCA protein assay kit (Keygentec), and equal amount of protein was loaded in each lane. Constant voltage electrophoresis was carried out with 10% polyacrylamide gels. Then the proteins were transferred to polyvinylidene fluoride (PVDF) membranes (Merk, Massachusetts, USA). PVDF membranes were blocked with 3% bovine serum albumin (BSA) (Sigma) and hybridized with anti-FoxP3 antibody (1:1000) (ab450, Abcam, Cambridge, UK), anti-GSK3β antibody (1:1000) (ab93926, Abcam), anti-β-catenin antibody (1:1000) (ab6302, Abcam), and anti-β-actin antibody (1:2000) (ab8226, Abcam) overnight at 4 ˚C. After washed with TBST (Tris-buffered saline and Tween 20) (Keygentec), the PVDF membrane were incubated with secondary antibodies (PV9000, ZSGB-bio, Beijing, China) at room temperature for 60 minutes, followed by washing with TBST. Finally, PVDF membranes were covered with 3, 3-Diaminobenzidine (DAB) (ZLI-9017, ZSGB-bio) for the display of specific protein bands.

Tumor-sphere formation assay

MHCC-LM3 cells from control and co-culture groups were trypsinized into single cells and resuspended in TICs medium consisting of DMEM/F-12 (Invitrogen) supplemented with epidermal growth factor (PHG0311, Gibco), basic fibroblast growth factor (PHG0266, Gibco), insulin (41400045, Gibco), B27 (17504044, Gibco). The cells were seeded at a density of 1×10^4 cells/well in ultra-low attachment 6-well plates. After 21 days of culture with replenishment of one half of the medium every 3 days, tumor spheres were observed and count.

In vivo tumorigenesis assay

All animal experiments were approved by the Institutional Animal Care and Use Committee of Dalian Medical University. Male BALB/c nude mice, 4–6 weeks of age, were used in this study. 5×10^6 cells harvested from ALG beads before and after co-cultured with Tregs were suspended in 100 μl saline supplement with 50% Matrigel (BD Biosciences) respectively, and then injected subcutaneously into the dorsal flanks of mice. Each experimental group included five mice. Animals were sacrificed after 6 weeks, and tumor volume (cm^3) was measured weekly using electronic calipers and calculated with the formula (length × width ×height) × Π/2.

Tregs-derived exosomes isolation and identification

Exosomes were isolated from the culture supernatant of Tregs by using a Total Exosome Isolation Reagent (4478359, Invitrogen), followed the manufacturer's instructions. The exosome morphology was observed by transmission electron microscopy (TEM) (JEM1230, JEOL, Japan). The particle size and exosome concentration were determined by nanoparticle tracking analysis (NTA) (NanoSight NS300, Malvern, UK). Then characterized by flow cytometry analysis of exosome surface markers CD63 (10606D, Thermo Fisher Scientific) and CD81 (10622D, Thermo Fisher Scientific). Mouse IgG1 was used as an isotype control.

DiO staining of Tregs-derived exosomes

10 μg of exosomes were incubated with lipophilic tracer DiO solution (Thermo Fisher Scientific) for 20 min at 37 °C. Excessive DiO was removed with Exosome Spin Columns (MW 3000) (Thermo Fisher Scientific). DiO-labeled exosomes (5 μg) were added to the culture media of the ALG-MHCC-LM3 cells.

Statistical analysis

All individual experiments were performed at least three times, with three replicates. Data were expressed as means ± standard deviation (SD). The significance of differences between two groups was determined using unpaired Student's t-tests. Differences were considered significant at $P < 0.05$.

Results

Tregs isolation and characterization

$CD4^+CD25^+CD127^-$ cells were isolated and expanded in vitro (Figure 1a), nearly 93% of cells were CD4 positive, besides, among $CD4^+$ cells, 98% were CD25 and FoxP3 double positive Tregs (Figure 1b).

Tregs enhanced the stemness of HCC cells

After 3 days of co-culture (Figure 1c), $CD133^+$ HCC cells increased significantly (P=0.0125), from 9.856% ± 3.264% to 31.324% ± 6.134% (Figure 1d). Besides, TICs related genes CD133 (P=0.0119), Oct3/4 (P=0.0241), Sox2 (P=0.0024), c-Myc (P=0.0133), Klf4 (P=0.0348), Nanog (P=0.0015), CD13 (P=0.0104), and EpCAM (P=0.0396) were significantly upregulated (Figure 1e). In addition, E-cadherin (P=0.0177) was

down-regulated, N-cadherin (P=0.0120) and vimentin (P=0.0191) were up-regulated after co-cultured with Tregs (Figure 1f), which indicated Tregs induced the EMT of HCC cells to acquire TIC characteristics. Moreover, β-catenin and its downstream gene c-Myc were significantly increased in HCC cells after co-culture (Figure 1g).

Tumor sphere formation and tumorigenesis assay were performed to further confirm the enhancement of HCC stemness. After co-cultured with Tregs, HCC cells formed more compact spheres (Figure 2a) as well as larger tumors in nude mice (P=0.0386) (Figure 2b-c).The above results verified that Tregs enhanced the stemness of HCC cells.

Tregs activated Wnt/β-catenin pathway to promote HCC TIC characteristics

After treatment with Wnt pathway inhibitor XAV-939 during co-culture, β-catenin was significantly decreased (Figure 3a), and TICs related genes Oct3/4 (P=0.0225), Nanog (P=0.0139), CD133 (P=0.0126), SOX2 (P=0.0378), c-Myc (P=0.0381), Klf4 (P=0.0420) were down-regulated significantly compared to control (Figure 3b). In addition, $CD133^+$ cells ratio remarkably decreased from 31.324 ± 6.134 to 3.024 ± 1.287 (P=0.0098) (Figure 3c-d).

Tregs enhanced HCC stemness through exosomes

Exosomes isolated from the conditioned medium of Tregs had typical morphology and size (Figure 4a), which were verified to express the exosomal markers CD63 and CD81 (Figure 4b).

After co-cultured with Tregs-derived exosomes (stained with Dio) (Figure 4c), TICs related genes Oct3/4 (P=0.0359), Nanog (P=0.0122), CD133 (P=0.0118), SOX2 (P=0.0184), c-Myc (P=0.0218), Klf4 (P=0.0415) were significantly up-regulated (Figure 4d), $CD133^+$ TICs ratio increased from 9.856 ± 3.264 to 27.983 ± 7.147 (0.0211) (Figure 4e-f), and β-catenin along with c-Myc were increased as well (Figure 4g) in HCC cells. When 10 μM GW4869 was added during co-culture to inhibit Tregs exosomes release, as expected, β-catenin as well as HCC TICs related genes Oct3/4 (P=0.0113), Nanog (P=0.0092), CD133 (P=0.0208), SOX2 (P=0.0312), c-Myc (P=0.0255) were significantly down-regulated (Figure 4h-i), and $CD133^+$ TICs ratio decreased from 31.324 ± 6.134 to 8.643 ± 3.866 (P=0.0142) (Figure 4j-k). The results indicated that Tregs enhanced HCC stemness through exosomes.

Lower expression of FoxP3 promoted Wnt/β-catenin pathway to enhance HCC stemness

It was found that FoxP3 was lower expressed in HCC tissue compared to that in paratumor tissue, in contrast, CD133 level was higher in tumor tissue (Fig. S1). After co-cultured with Tregs-derived exosomes, FoxP3 and GSK3β were both significantly down-regulated in HCC cells (Fig. S2). Furthermore, forced expression of FoxP3 (P=0.0209) led to higher expression GSK3β while lower expression of β-catenin in HCC cells (Figure 5a-b). In addition, $CD133^+$ TICs ratio decreased from 3.863 ± 1.730 to 1.145 ± 0.423 (P=0.0421) after forced expression of FoxP3 (Figure 5c-d).

Accordingly, FoxP3 interference (P=0.0298, P=0.0334, P=0.0387) (Figure 6a-b) led to decreased GSK3β, increased β-catenin (Figure 6b), and subsequent higher $CD133^+$ TICs ratio (Figure 6c), from 3.090 ± 0.973 to 7.329 ± 0.521 (P=0.0271) (Figure 6d). These results suggested Tregs activated Wnt/β-catenin pathway and enhanced HCC stemness through down-regulation of FoxP3.

Discussion

Accumulating evidence indicates that HCC therapeutic resistance and recurrence are closely associated with cancer stem cells (CSCs), or TICs [7,8]. Tregs function as dominant inhibitory components in the immune microenvironment of HCC, which are undisputed to be associated with the invasiveness of HCC, and are a promising independent predictor of recurrence and survival in HCC patients [9,10].

A few studies have reported the ability of Tregs to drive the tumor cells to be TICs. Yang et al. found $Foxp3^+$ IL-17^+Treg cells induced colorectal cancer cells to up-regulated TICs related markers including CD133, CD44s, CD166, EpCAM, and ALDH1 [11]. Xu et al. disclosed that Tregs upregulated the stemness property of breast cancer cells through increasing the side-population, promoting tumor sphere formation, enhancing the expression of stemness genes including Sox2, Nanog, Oct3/4 [12]. In this study, for the first time, we found that Tregs enhanced the stemness of HCC cells, demonstrated by increased TICs ratio, upregulated expression of TICs related genes CD133, Oct3/4, Sox2, c-Myc, Klf4, Nanog, CD13, EpCAM, elevated tumor sphere formation and tumorigenic ability.

FoxP3 was initially identified as a “switch” for the development and function of Tregs, and thought to be restricted to hematopoietic tissues. Recently, reports had demonstrated that FoxP3 was also expressed in tumor cells, suggesting that FoxP3 might have a broader role in cancer. However, the biological function and clinical relevance of FoxP3 in tumor cells remain controversial. Some studies found that FoxP3 expression levels elevated in a number of tumor cell types, and indicated tumor progression [13–15]. While others reported FoxP3 as cancer suppressor gene in breast cancer [16,17], prostate cancer [18], gastric cancer [19], as well as HCC [20]. Shi et al. found that high expression of FoxP3 significantly correlated with early TNM stage, better survival and reduced recurrence. Additionally, they demonstrated FoxP3 suppressed the proliferation and invasion of HCC cells in vitro and reduce tumor growth in vivo [20]. In this study, we found FoxP3 expression in tumor tissue was significantly lower than that in paratumor tissue, while CD133 was significantly higher in tumor tissue compared to paratumor tissue. In addition, forced expression of FoxP3 led to significantly lower number of HCC TICs, and in contrast, FoxP3 inhibition significantly increased the HCC TICs. These results were in accordance with Liu et al., which showed FoxP3 was significantly down-regulated in cancer stem cell-like cells of colorectal cancer, and forced expression of FoxP3 significantly decreased self-renewal ability of cancer stem cells including the side population, cancer stem cell marker CD133, colonosphere formation ability in vitro, and tumor formation ability in vivo [21].

Abnormal initiation of Wnt/β-catenin pathway has been recognized in HCC TICs [22]. After co-cultured with Tregs, GSK3β was significantly down-regulated and β-catenin and c-Myc were significantly upregulated in HCC cells. Moreover, after Wnt/β-catenin pathway was inhibited, TIC related genes as well as TICs ratio were significantly decreased.

Exosomes are secreted extracellular membrane vesicles, serve as vehicles for transfer cytosolic proteins, lipids, and nucleotides including non-coding RNAs between cells [23]. It was reported Tregs-derived exosomes could suppress immune cell proliferation and cytokine secretion to assist Tregs-mediated immune suppression [24]. Nonetheless, the role Tregs-derived exosomes play in regulating tumor cell behavior remains poorly understood. This study, for the first time, showed Tregs-derived exosomes significantly up-regulated TICs related genes, and increased $CD133^+$ TICs ratio in HCC cells. Furthermore, lower FoxP3, GSK3β and higher β-catenin, c-Myc were found in HCC cells after co-cultured with Tregs-derived exosomes. And which were reversible by inhibition of exosomes release.

Though the experimental design of this study was formulated and executed after thorough consideration and literature search, there exist several limitations that need to be mentioned. First of all, weather GSK3β was the direct target of FoxP3 was unrevealed. Secondly, the correlation of FoxP3 expression with the metastasis, relapse, and overall survival of HCC patients should be investigated to further confirm the tumor suppressor role of FoxP3 in HCC. Thirdly, the detailed regulatory mechanism by which Tregs-derived exosomes enhance HCC cell stemness was undefined. LncRNAs (long non-coding RNAs) or miRNAs or other components in Tregs-derived exosomes responsible for affecting HCC stemness should be identified in further studies.

Conclusions

In summary, this study reported Tregs, through their exosomes, suppressed FoxP3, GSK3β and activated β-catenin to enhance the stemness of HCC. It was the first study to show that Tregs regulated HCC TIC characteristics.

Abbreviations

TICs
tumor initiating cells
HCC
hepatocellular carcinoma
Tregs
regulatory T cells
EMT
epithelial to mesenchymal transition
LncRNAs
long non-coding RNAs

Declarations

Ethics approval and consent to participate

The use of human peripheral blood was reviewed and approved by the Ethics Committee of Dalian Municipal Central Hospital.

Consent for publication

Not applicable

Availability of data and materials

The dataset(s) supporting the conclusions of this article is(are) available in the figshare repository [https://doi.org/10.6084/m9.figshare.11894658.v1].

Competing interests

The authors declare that they have no competing interests

Authors' contributions

All authors contributed to the study conception and design. Material preparation, data collection and analysis were performed by CL, YYP, JJ, YYW, HSW, YYG. LZ and CL were major contributors in writing the manuscript. All authors read and approved the final manuscript.

Funding

This work is supported by "Young star of science and technology" of Dalian Science and Technology Bureau, grant no. 2018RQ43.

Acknowledgements

Not applicable

References

1. Bray F, Ferlay J, Soerjomataram I, Siegel RL, Torre LA, Jemal A. Global cancer statistics 2018: GLOBOCAN estimates of incidence and mortality worldwide for 36 cancers in 185 countries. CA Cancer J Clin. 2018;68:394–424.
2. Lai HH, Li CW, Hong CC, et al. TARBP2-mediated destabilization of Nanog overcomes sorafenib resistance in hepatocellular carcinoma. Mol Oncol. 2019;13:928–45.
3. Kang Q, Gong J, Wang M, Wang Q, Chen F, Cheng KW. 6-C-(E-Phenylethenyl)Naringenin Attenuates the Stemness of Hepatocellular Carcinoma Cells by Suppressing Wnt/beta-Catenin Signaling. J Agric

Food Chem. 2019;67:13939–47.
4. Langhans B, Nischalke HD, Kramer B, et al. Role of regulatory T cells and checkpoint inhibition in hepatocellular carcinoma. Cancer Immunol Immunother. 2019;68:2055–66.
5. Fu J, Xu D, Liu Z, et al. Increased regulatory T cells correlate with CD8 T-cell impairment and poor survival in hepatocellular carcinoma patients. Gastroenterology. 2007;132:2328–39.
6. Wang Y, Liu T, Tang W, et al. Hepatocellular Carcinoma Cells Induce Regulatory T Cells and Lead to Poor Prognosis via Production of Transforming Growth Factor-beta1. Cell Physiol Biochem. 2016;38:306–18.
7. Chen J, Jin R, Zhao J, et al. Potential molecular, cellular and microenvironmental mechanism of sorafenib resistance in hepatocellular carcinoma. Cancer Lett. 2015;367:1–11.
8. Ishiguro K, Yan IK, Lewis-Tuffin L, Patel T. Targeting Liver Cancer Stem Cells Using Engineered Biological Nanoparticles for the Treatment of Hepatocellular Cancer. Hepatol Commun. 2020;4:298–313.
9. Hassan EA, Ahmed EH, Nafee AM, El-Gafary N, Hetta HF, El-Mokhtar MA. Regulatory T. Cells, IL10 and IL6 in HCV Related Hepatocellular Carcinoma after Transarterial Chemoembolization (TACE). Egypt J Immunol. 2019;26:69–78.
10. Liu Q, Du F, Huang W, et al. Epigenetic control of Foxp3 in intratumoral T-cells regulates growth of hepatocellular carcinoma. Aging. 2019;11:2343–51.
11. Yang S, Wang B, Guan C, et al. Foxp3 + IL-17 + T cells promote development of cancer-initiating cells in colorectal cancer. J Leukoc Biol. 2011;89:85–91.
12. Xu Y, Dong X, Qi P, et al. Sox2 Communicates with Tregs Through CCL1 to Promote the Stemness Property of Breast Cancer Cells. Stem Cells. 2017;35:2351–65.
13. Merlo A, Casalini P, Carcangiu ML, et al. FOXP3 expression and overall survival in breast cancer. J Clin Oncol. 2009;27:1746–52.
14. Grimmig T, Kim M, Germer CT, Gasser M, Waaga-Gasser AM. The role of FOXP3 in disease progression in colorectal cancer patients. Oncoimmunology. 2013;2:e24521.
15. Zeng C, Yao Y, Jie W, et al. Up-regulation of Foxp3 participates in progression of cervical cancer. Cancer Immunol Immunother. 2013;62:481–7.
16. Zuo T, Wang L, Morrison C, et al. FOXP3 is an X-linked breast cancer suppressor gene and an important repressor of the HER-2/ErbB2 oncogene. Cell. 2007;129:1275–86.
17. Zuo T, Liu R, Zhang H, et al. FOXP3 is a novel transcriptional repressor for the breast cancer oncogene SKP2. J Clin Invest. 2007;117:3765–73.
18. Wang L, Liu R, Li W, et al. Somatic single hits inactivate the X-linked tumor suppressor FOXP3 in the prostate. Cancer Cell. 2009;16:336–46.
19. Ma GF, Chen SY, Sun ZR, et al. FoxP3 inhibits proliferation and induces apoptosis of gastric cancer cells by activating the apoptotic signaling pathway. Biochem Biophys Res Commun. 2013;430:804–9.

20. Shi JY, Ma LJ, Zhang JW, et al. FOXP3 Is a HCC suppressor gene and Acts through regulating the TGF-beta/Smad2/3 signaling pathway. BMC Cancer. 2017;17:648.
21. Liu S, Zhang C, Zhang K, et al. FOXP3 inhibits cancer stem cell self-renewal via transcriptional repression of COX2 in colorectal cancer cells. Oncotarget. 2017;8:44694–704.
22. Guo JC, Yang YJ, Zheng JF, et al. Silencing of long noncoding RNA HOXA11-AS inhibits the Wnt signaling pathway via the upregulation of HOXA11 and thereby inhibits the proliferation, invasion, and self-renewal of hepatocellular carcinoma stem cells. Exp Mol Med. 2019;51:142.
23. Wang L, Wang C, Jia X, Yu J. Circulating Exosomal miR-17 Inhibits the Induction of Regulatory T Cells via Suppressing TGFBR II Expression in Rheumatoid Arthritis. Cell Physiol Biochem. 2018;50:1754–63.
24. Okoye IS, Coomes SM, Pelly VS, et al. MicroRNA-Containing T-Regulatory-Cell-Derived Exosomes Suppress Pathogenic T Helper 1 Cells. Immunity. 2014;41:503.

Figures

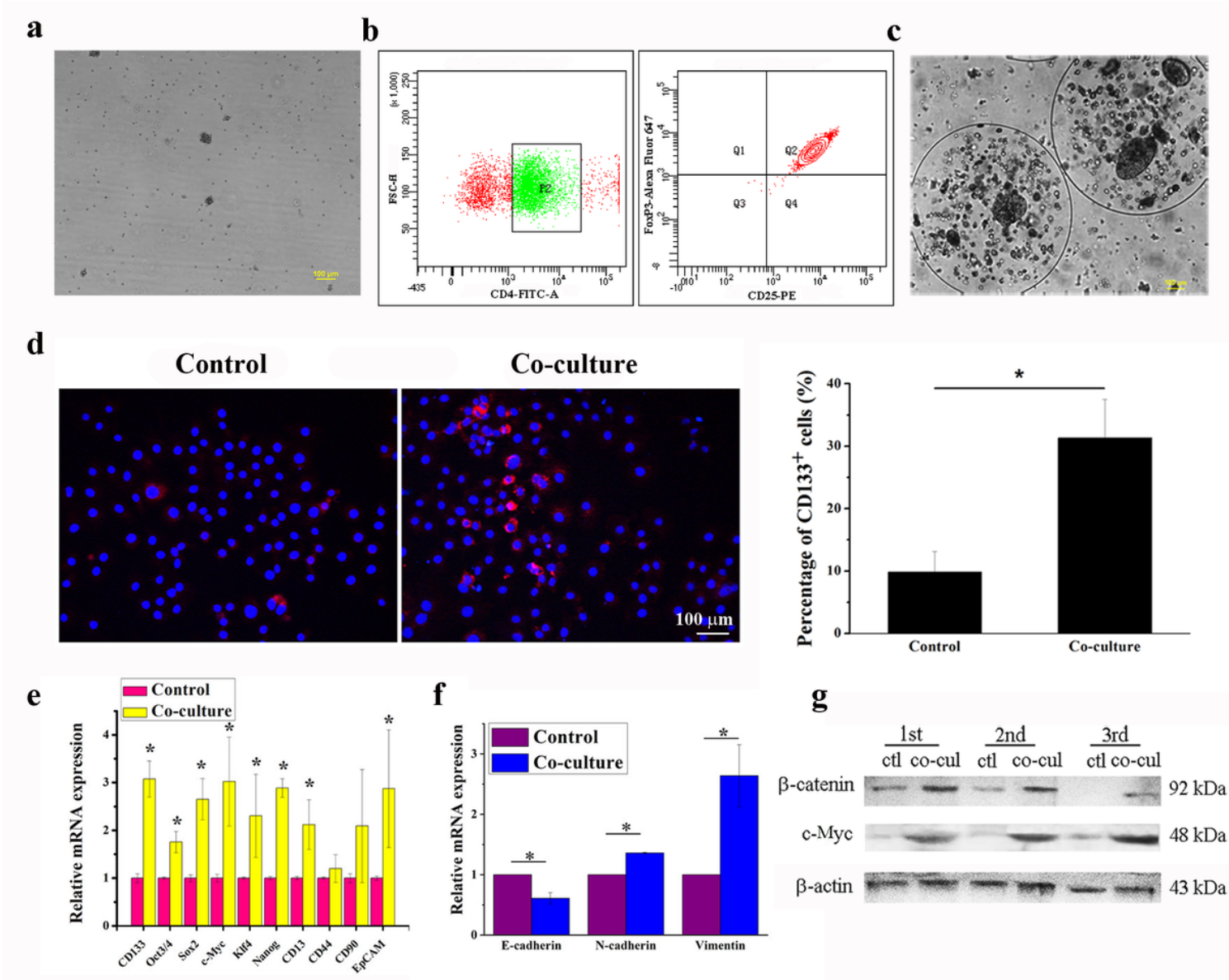

Figure 1

Tregs enhanced HCC stemness. (A) CD4+CD25+CD127- cells isolation and in vitro expansion. (B) Flow cytometry analysis of CD4, CD25, and FoxP3 expression in Tregs. (C) Co-culture of MHCC-LM3 cells and Tregs. (D) Immunofluorescence staining of CD133 (labled with Alxa 555 conjugate antibody) and nucleus (labeled with Hoechst 33342) of MHCC-LM3 cells, and CD133+ TICs ratio before and after co-cultured with Tregs, * $P < 0.05$, compared with control group. (E) RT-qPCR analysis of TICs related genes CD133, Oct3/4, Sox2, c-Myc, Klf4, Nanog, CD13, and EpCAM expression, * $P < 0.05$, compared with control group. (F) EMT-related genes E-cadherin, N-cadherin, and Vimentin expression, * $P < 0.05$, compared with control group. (G) Western blot analysis of β-catenin and c-Myc in MHCC-LM3 cells before and after co-cultured with Tregs

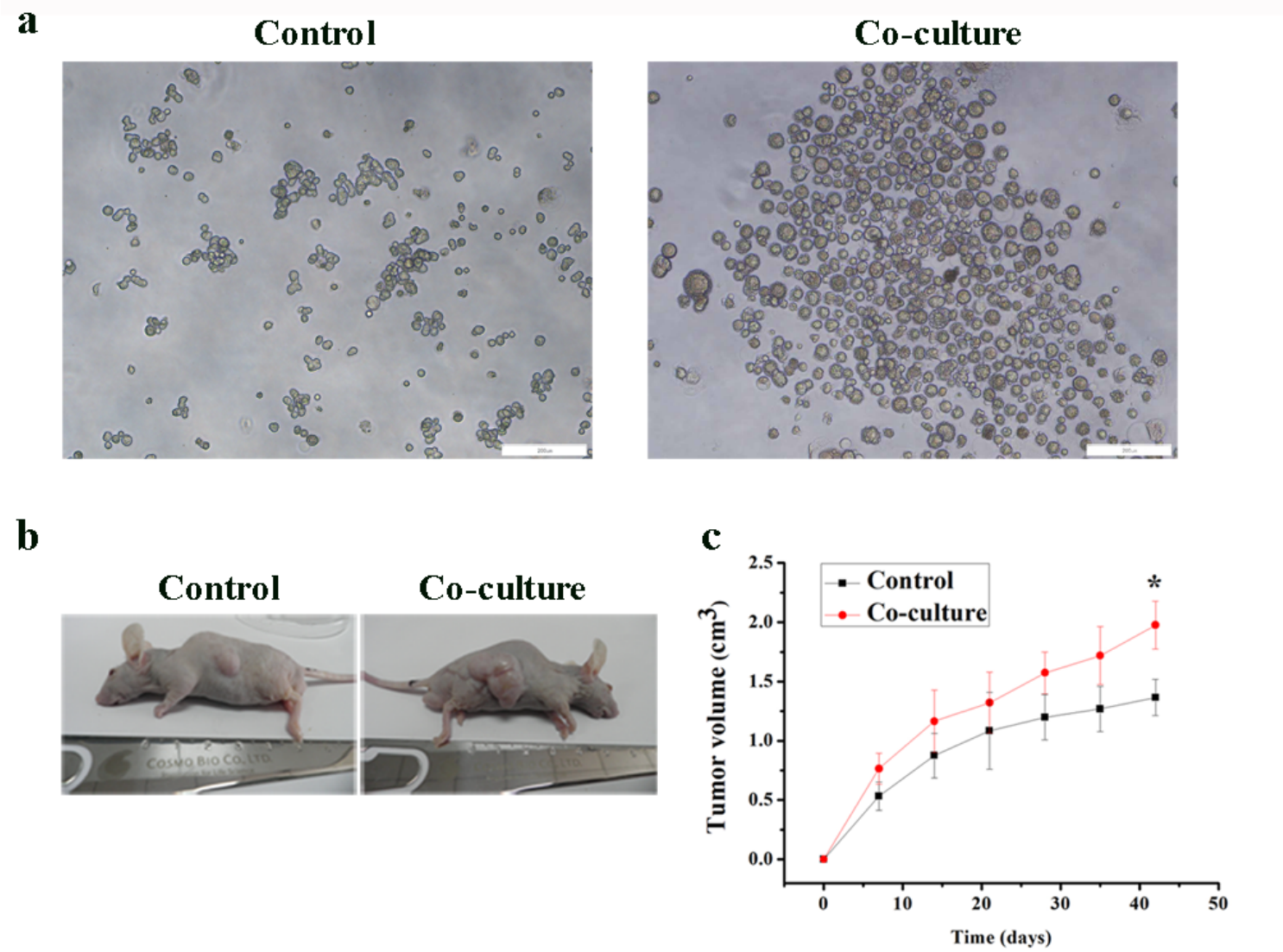

Figure 2

Tregs enhanced sphere formation ability and tumorigenicity of HCC cells. (a) In vitro sphere formation ability of MHCC-LM3 cells before and after co-cultured with Tregs, bar: 500 μm. (b) In vivo tumorigenicity of MHCC-LM3 cells before and after co-cultured with Tregs. (c) Tumor volume change in nude mice after subcutaneously injected with 5×106 MHCC-LM3 cells for 6 weeks, * $P < 0.05$, compared with control group

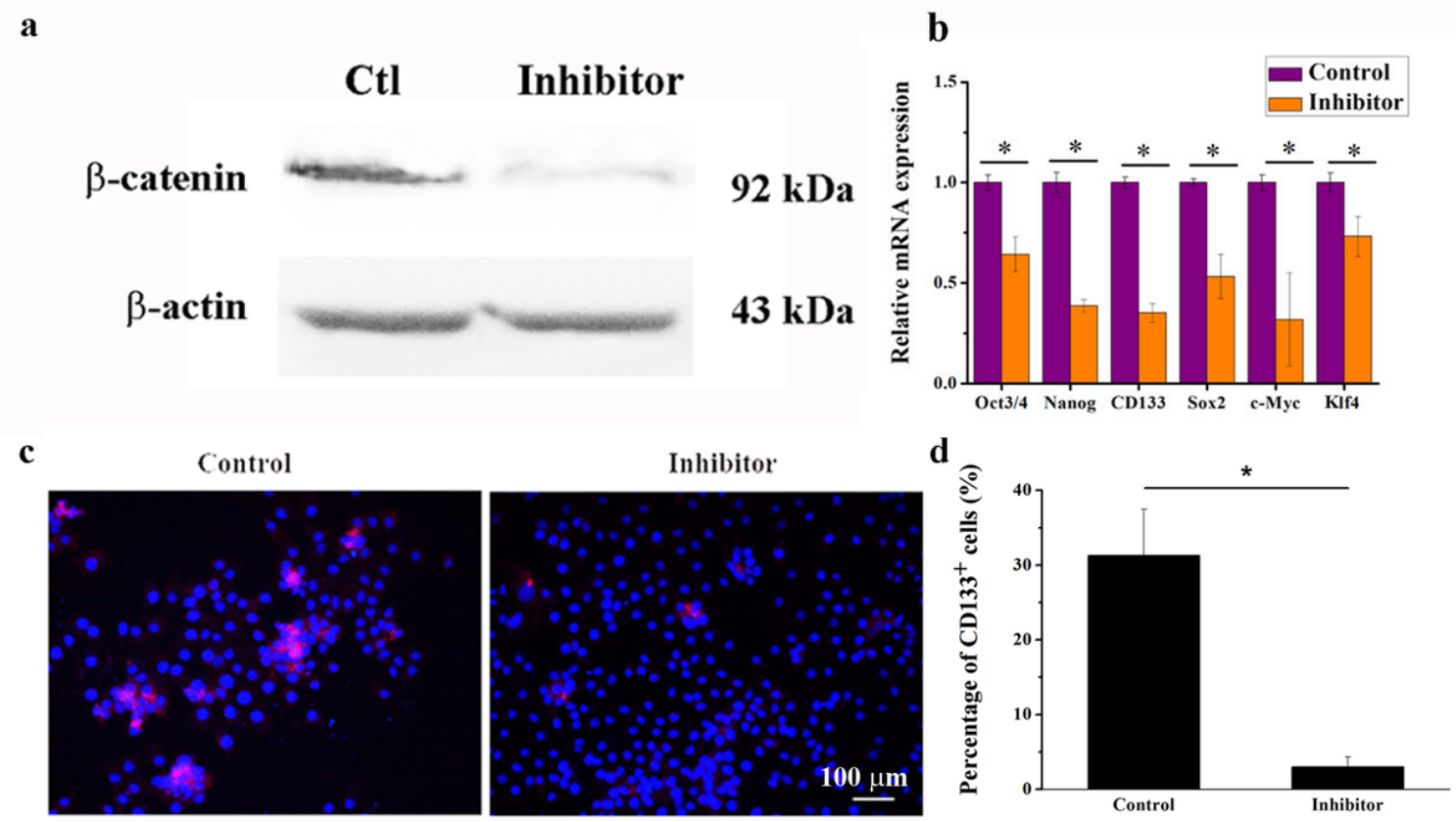

Figure 3

Tregs promoted HCC TICs characteristics through Wnt/β-catenin pathway. (a) Western blot analysis of β-catenin in MHCC-LM3 cells with or without 5 μM XAV-939 during co-culture. (b) RT-qPCR analysis of TICs related genes Oct3/4, Nanog, CD133, Sox2, c-Myc, Klf4 expression after treatment with 5 μM XAV-939 during co-culture, * $P < 0.05$, compared with control group (co-culture without XAV-939). (c) Immunofluorescence staining of CD133 (labled with Alxa 555 conjugate antibody) and nucleus (labeled with Hoechst 33342) of MHCC-LM3 cells after treatment with 5 μM XAV-939. (D) CD133+ TICs ratio with or without 5 μM XAV-939, * $P < 0.05$, compared with control group

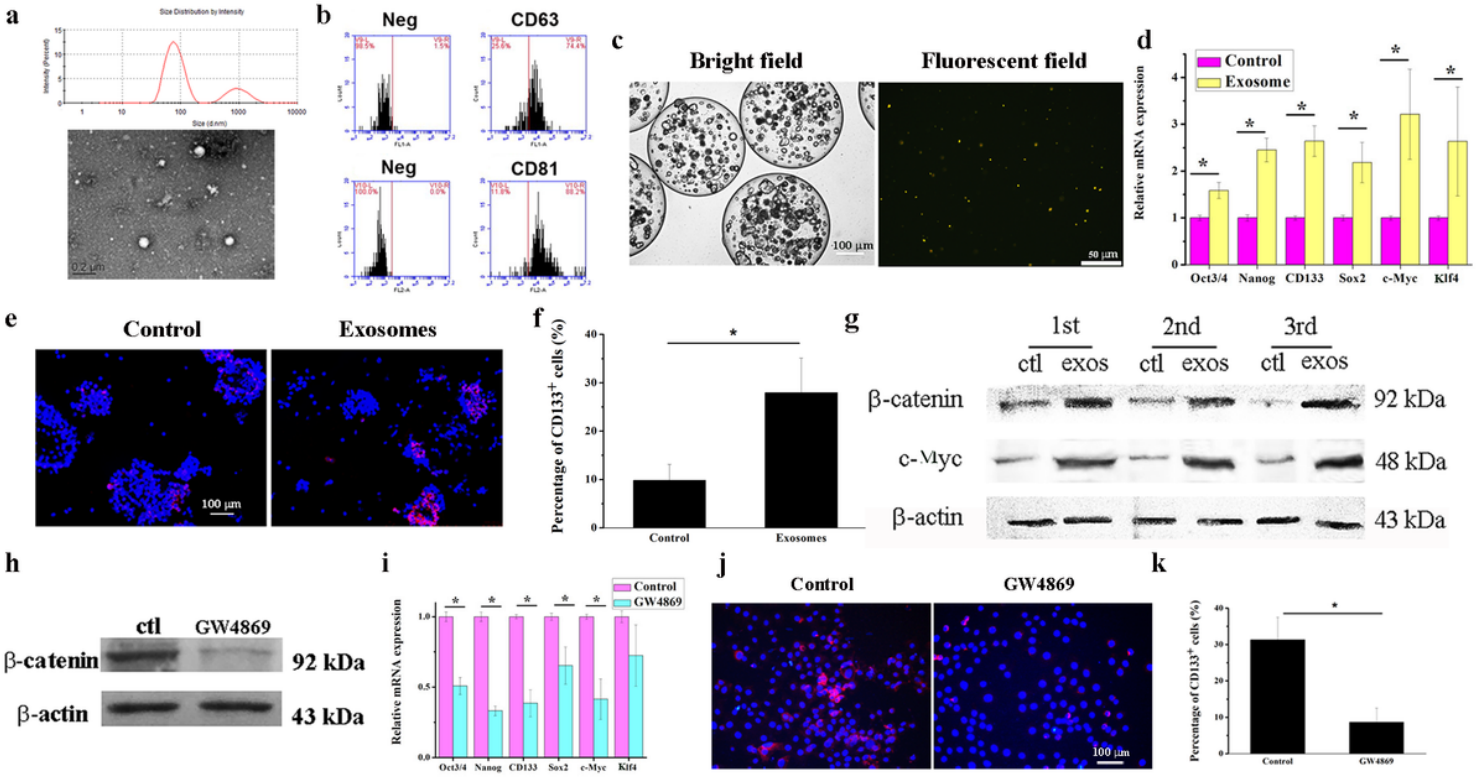

Figure 4

Tregs enhanced HCC stemness through exosomes. (a) NTA analysis of size distribution and TEM analysis of morphology of Tregs-derived exosomes. (b) Flow cytometry analysis of exosomal markers CD63 and CD81, mouse Ig G was used as isotype control. (c) Bright and fluorescent field images of MHCC-LM3 cells encapsulated in calcium alginate co-cultured with Tregs-derived exosomes (labeled with DiO). (d) RT-qPCR analysis of Oct3/4, Nanog, CD133, Sox2, c-Myc, Klf4 mRNA before and after co-cultured with Tregs-derived exosomes, * $P < 0.05$, compared with control group. (e) Immunofluorescence staining of CD133 (labled with Alxa 555 conjugate antibody) and nucleus (labeled with Hoechst 33342) of MHCC-LM3 cells before and after co-cultured with Tregs-derived exosomes. (f) CD133+ TICs ratio change after co-cultured with Tregs-derived exosomes, * $P < 0.05$, compared with control group. (g) Western blot analysis of β-catenin and c-Myc in MHCC-LM3 cells before and after co-cultured with Tregs-derived exosome. (h) Western blot analysis of β-catenin of HCC cells after treated with 10 μM exosome inhibitor GW4869 during co-culture. (i) RT-qPCR analysis of Oct3/4, Nanog, CD133, Sox2, c-Myc, Klf4 mRNA after treated with GW4869 during co-culture, * $P < 0.05$, compared with control group (co-culture without GW4869). (j) Immunofluorescence staining of CD133 (labled with Alxa 555 conjugate antibody) and nucleus (labeled with Hoechst 33342) of MHCC-LM3 cells after before and after treated with GW4869 during co-culture. (k) CD133+ TICs ratio after treated with GW4869 during co-culture, * $P < 0.05$, compared with control group.

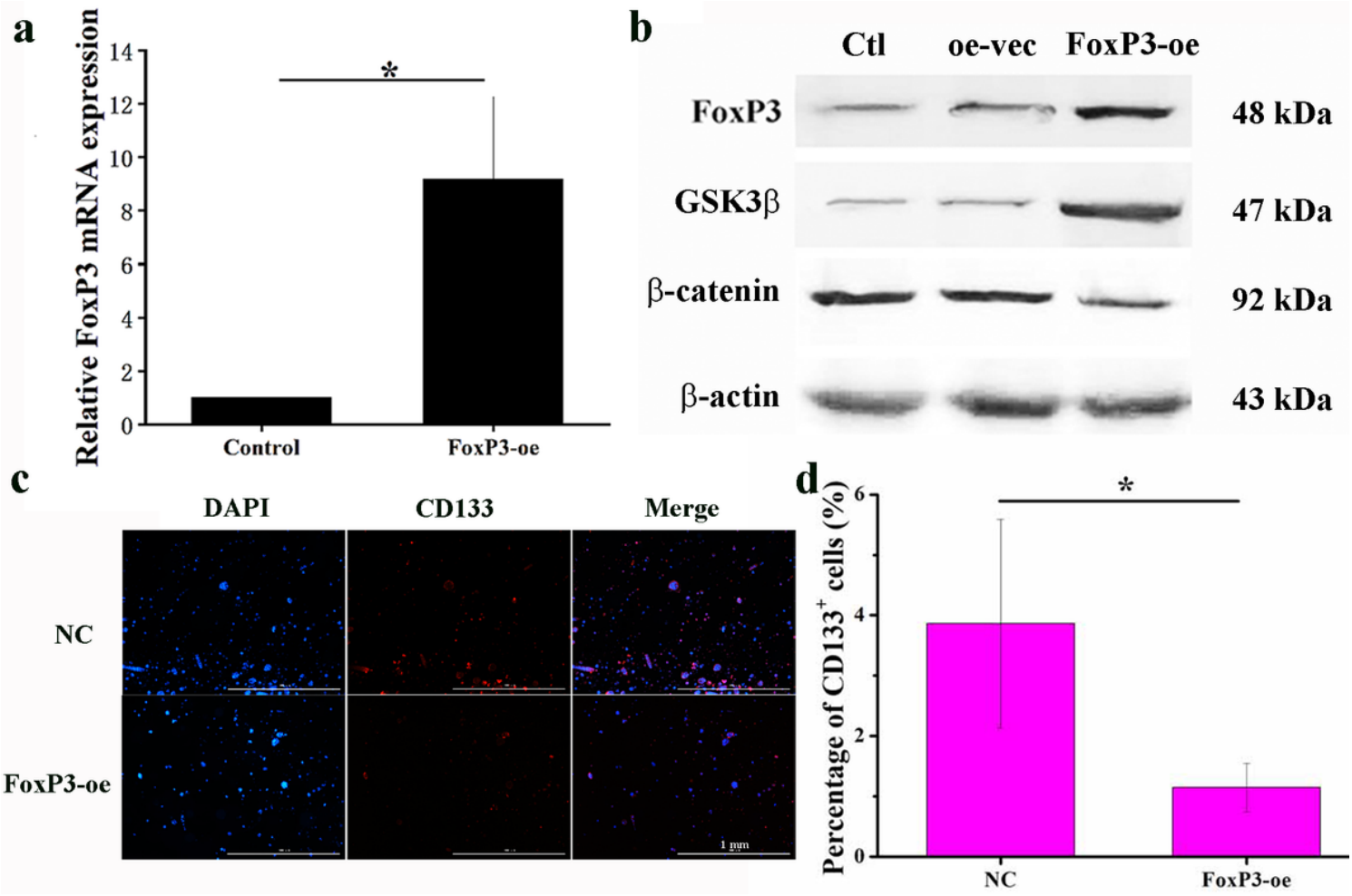

Figure 5

FoxP3 overexpression inhibited HCC TICs characteristics. (a) RT-qPCR analysis of FoxP3 mRNA expression in MHCC-LM3 cells after forced expression of FoxP3. (b) Western blot analysis of FoxP3, GSK3β and β-catenin in MHCC-LM3 cells after forced expression of FoxP3. (c) Immunofluorescence staining of CD133 (labled with Alxa 555 conjugate antibody) and nucleus (labeled with Hoechst 33342) of MHCC-LM3 cells after forced expression of FoxP3. (d) CD133+ TICs ratio change after forced expression of FoxP3, * $P < 0.05$, compared with control group (empty vector).

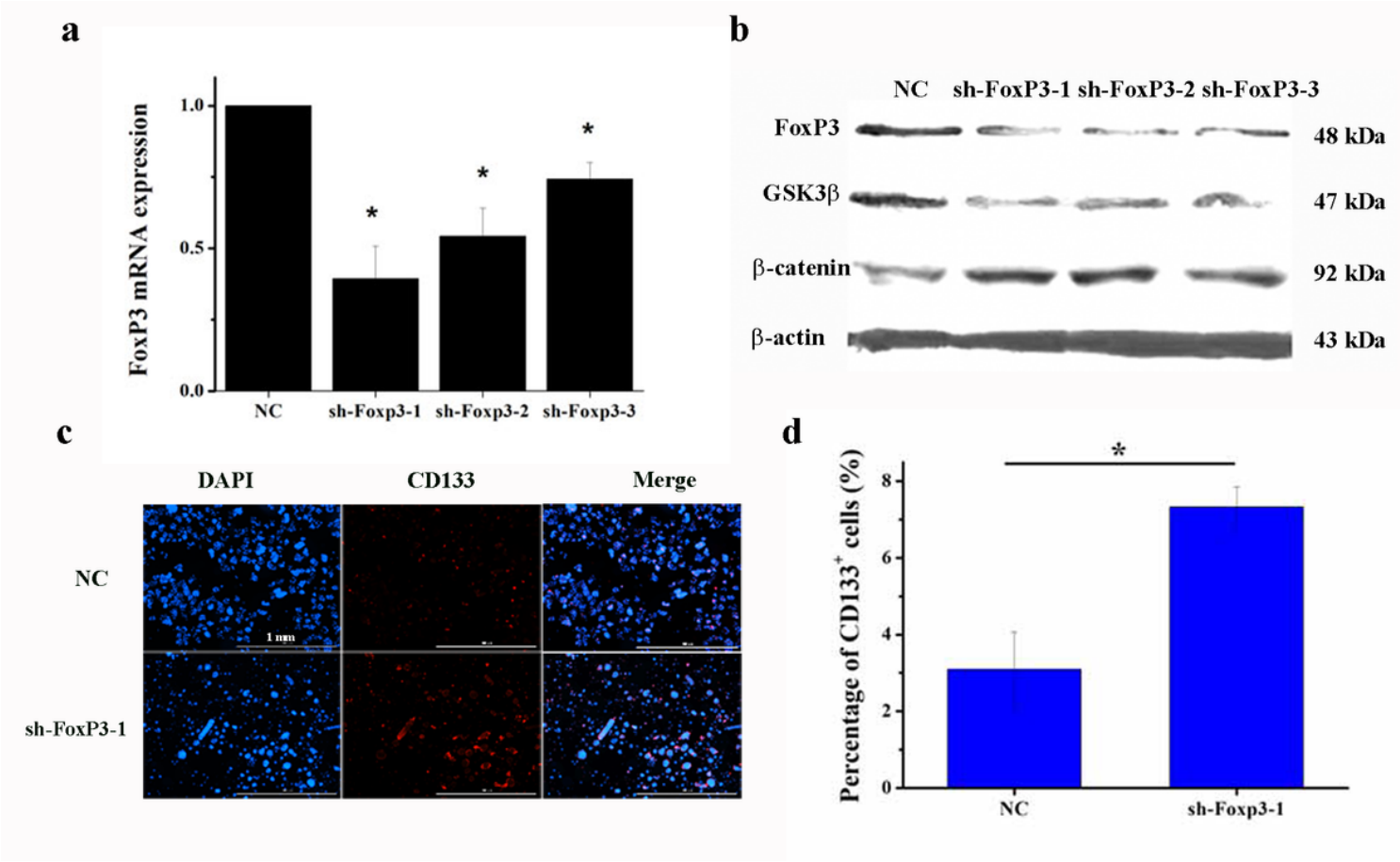

Figure 6

FoxP3 interference enhanced HCC stemness. (a) RT-qPCR analysis of FoxP3 mRNA in MHCC-LM3 cells after three shRNAs transfection, * $P < 0.05$, compared with control group (scramble shRNA). (b) Western blot analysis of FoxP3, GSK3β and β-catenin in MHCC-LM3 cells after FoxP3 interference. (c) Immunofluorescence staining of CD133 (labled with Alxa 555 conjugate antibody) and nucleus (labeled with Hoechst 33342) of MHCC-LM3 cells after FoxP3 interference with sh-FoxP3-1. (d) CD133+ TICs ratio change after FoxP3 interference with sh-FoxP3-1, * $P < 0.05$, compared with control group.

Supplementary Files

This is a list of supplementary files associated with this preprint. Click to download.

- FigS1.tif
- FigS2.tif
- TableS.docx